Journal of Asian Ceramic Societies 4 (2016) 143–148

HOSTED BY

Contents lists available at ScienceDirect

Journal of Asian Ceramic Societies

journal homepage: www.elsevier.com/locate/jascer

Experimental study on performance of imitative RPC for sulphate leaching

Xu-guang Tang [a,b,*], You-jun Xie [a,b], Guang-cheng Long [a,b]

[a] School of Civil Engineering and Architecture, Central South University, Changsha 410075, China
[b] School of Civil Engineering, Science and Technology University of Hunan, Xiangtan 411201, China

ARTICLE INFO

Article history:
Received 13 May 2015
Received in revised form
25 November 2015
Accepted 12 January 2016
Available online 5 February 2016

Keywords:
Imitative RPC material
Tunnel lining concrete
Properties to sulphate sodium solution leaching
Environment-friendly material

ABSTRACT

This paper presents a manufacturing process to make an imitative RPC material. The blend was regularly composed of cement, silica fume, and certain content of rubber powder. The granular size distribution of dry blend was optimized to reduce the porosity of set material and the imitative RPC material was characterized by high silica fume content and with very low water to binder ratio. Furthermore, fine crushed aggregate and local natural medium crude sand were used to form mineral skeleton. Properties of various reference concrete series were investigated by conducting multiple tests, including permeability and mechanical strength test, the salt solution absorption test, the accelerated sulphate attack test, etc. The results show that the imitative RPC is an environmental-friendly civil engineering material which owns favorable mechanical strength, high impermeability and qualified excellent durability in sulphate contained environment.

1. Introduction

In 1990s, Richard Pieer acquired a new concrete material by imitating the DSP materials [1,2], and its main content was active powders, naming the reactive powder concrete [3,4]. Because of its high strength and excellent performance on durability, RPC created extensive application in producing various entity projects and incredibly strong prefabrications with high durability. For example, the world's first pedestrian/bicycle bridge was built with RPC 200 materials [5,6]. In Seoul, Korea an arch bridge with span of 125 m has been constructed by using RPC 200 in 2002 [7,8]. United States has completed the first high-grade RPC single-span simply supported girder bridge in 2006 [9]. Generally, the common RPC is more expensive than traditional materials for special technologies applied in preparation procedures and with high content of expensive materials in preparation. For example, coarse aggregates were removed and replaced with graded quartz sands and addition of steel fibers to enhance flexibility, etc. There are some literatures showing that the steel fibers take up approximately half of the costs [10], and high content of pricey binder in per cube inevitably increases the manufacturing cost of RPC. This paper investigates the performance of mortar serials to sulphate attack with various cement-based binders and selects the ordinary Portland cement as binder electee. According to the principle of RPC, an imitative RPC material (abbrev. imit-RPC, the same as below) was acquired with the local natural medium crude sand, fine crushed limestone, a compounded binder of ordinary Portland cement, high content of silica fume and certain content of fly ash, etc. Besides, properties against sulphate attack were investigated by employing an accelerated method of leaching with high concentrated sodium sulphate solution, indexes such as chloride ion permeability and sulphate salt solution absorption were measured for engineering needs.

2. Experimental

2.1. Materials and specimens

Seven concrete series were selected to be references in this study. They were made from local aggregates and traditional materials except RPC 130 serial. The sand used is natural medium crude sand in I/II grading zone. The coarse aggregate used is crushed limestone with the size range from 5 mm to 10 mm. Silica fume with a specific surface area of 20,470 m^2/kg and an ultra-pulverized fly ash with a specific surface area of 780 m^2/kg bought from

* Corresponding author at: School of Civil Engineering and Architecture, Central South University, Changsha 410075, China. Tel.: +86 13873239138.
E-mail addresses: Tangxuguang2008@aliyun.com (X.-g. Tang), Xieyj@mail.csu.edu.cn (Y.-j. Xie), scc2005@csu.edu.cn (G.-c. Long).
Peer review under responsibility of The Ceramic Society of Japan and the Korean Ceramic Society.

http://dx.doi.org/10.1016/j.jascer.2016.01.007

Table 1
Detailed components of the binder (mass ratio, dimensionless).

Concrete serial		P.O 42.5	SAC 42.5	SF	UFA slag	Polymers
1	1 (1#, 5#)	100	–	–	–	–
	2 (2#)	–	100	–	–	–
2	1-1 (3#)	75	–	5	20	–
	1-1A (4#)	75	–	3	20	2
3	Imitative RPC (6#)	72	–	20	8	–
	RPC 130 (7#)	80	–	20	–	–

Xiangtan power plant were used. Rubber powder with 30–50 meshes grinding from waste tire are added to relieve strain. Tables 1 and 2 summarize the components of binder and concrete mixture. Those ingredients were mixed, stirred by a forcible mixer, and then cured in saturated limewater solution at $20 \pm 2\,^{\circ}C$ after demolded. Specimens with a size of 150 mm × 150 mm × 150 mm were cored and cut in a size of Ø100 mm × 50 mm for measuring penetrability. Cylinder specimens with a size of Ø100 mm × 150 mm were prepared, and the specimens were drilled with a power drill fitted with 50 mm diameter water flush diamond tipped barrels. The cavity of the specimens were blocked, sealed at the bottom with epoxy resin, and then filled with sulphate solution. The core cylinders were prepared for salt absorption tests. In addition, the selected experimental solution is 50,000/150,000 ppm sodium sulphate solution which is prepared by mixing pure sodium sulphate into distilled hot water and sit at $20 \pm 2\,^{\circ}C$ for 24 h.

2.2. Testing procedures

The particle size and distribution of the granular material were investigated by using Rise-2008 laser particle size analyzer. Permeability was measured according to ASTM C1202 method. Tolerance against sulphate attack was designed with an accelerated method by infiltrating in high content sodium sulphate solution. Specimens were undergoing unilateral leaching for 150,000 ppm sodium sulphate solution at 7 days age and stored in the creep room with a temperature at $20 \pm 2\,^{\circ}C$ and a relative humidity at 50–60%. At regular intervals, a set of specimens were selected to examine the mechanical strength and check the invasion profile. The splitting strength was measured according to Standard GB/T 50081-2002. Index of anti-erosion factor was expressed by the ratio of actual splitting strength of leaching solution with leaching pure water. The invasion profile check was performed with a vernier-caliper. Three points were checked along profile for each fracture. The invasion depth comes from the mean measured values of each group.

3. Results

3.1. Summary of optimization for dry binder

The composition optimization for cement-based materials was adopted beforehand to withstand sulphate attack. Each treatment group prepared with w/b = 0.4. Specimens were made of ordinary Portland cement (abbrev. P.O 42.5), ground Portland cement clinker (abbrev. clinker), sulphoaluminate cement (abbrev. SAC 42.5) and aluminous cement (abbrev. HAC 42.5). The fiducial group was plain cement mortar serial and the control group added with silica-aluminum materials. All specimens should be cured in a saturated limewater solution for 7 days after demolded, and then semi-immersed in 50,000 ppm sodium sulphate. The cumulative mass of crystal salt and the total mass variation (crystal salt and the prism) were checked with the same interval (described in Fig. 1). The results show that the mortar serial with HAC 42.5 accumulated the maximum mass of crystal salt, and its general order was HAC 42.5 > P.O 42.5 > clinker > SAC 42.5. When silica-aluminum materials replace portion of cement, the cumulative mass of crystal salt decreased and the crystal salt order was HAC 42.5 > SAC 42.5 > P.O 42.5 > clinker. Fig. 1(b) is the total variation of mortar specimens in sodium sulphate solution. It shows that the P.O 42.5 serial with silica-aluminum material increases by a wide margin of total mass during the first 30 days, and then moves to a slow increasing stage. The clinker serial and SAC 42.5 serial in control group have small growth on total mass of specimens. For HAC 42.5, both of the treatment groups have a high increasing ratio. In summary, a compound of Portland ordinary cement and the silica-aluminum materials was an electee binder for imitative RPC materials.

Besides the composition of binder contributing greatly to the hardened matrix, the particle size distribution has a significant influence on cement hydration process and its hardened paste. Therefore, a close-grained bulk density can be acquired by introducing a wide range of gradation, and its size-frequency of particles satisfies the Gaudin-Schuhmann Equation (see Eq. (3.1)). According to Gaudin-Schuhmann Equation, the granular material is sparsely packed when Fuller index is 0.5, and acquires the most dense packing at 0.33. In actual engineering, the granular materials can reach minimal fraction void when the Fuller index ranges from 0.33 to 0.50 [11].

$$P(d_i) = 100\left(\frac{d_i}{d_{\max}}\right)^n \tag{3.1}$$

where $P(d_i)$ is the percentage of minus sieve, d_i the current size, $d_{\max}$ the maximum particle diameter and n is the Fuller index.

The particle size and distribution of binder components were investigated by using Rise-2008 laser particle size analyzer. The test results show that cement particles distribution ranges from 0.2 μm to 60 μm and the ultra fine fly ash contain particles diameter from 0.2 μm to 5 μm. Silica fume particles distribute between 0.1 μm and 1.0 μm, and the average diameter is 0.12 μm. In Fig. 2, it can be seen that the size distribution of cement goes beyond the minimal fraction void region. The size distribution curve stands under the sparsely packing curve meaning that cement is short of fine particles. When partial cement is replaced by ultra fume ash and silica fume, the size distribution of particle is stretched greatly. From main pattern of Fig. 2, it can be found that the synthetic gradation of binder is optimized. When the binder composition is 72% of cement combined with 8% of ultra fume ash and 20% of silica fumes, its size distribution falls into the grading limits of reaching minimal fraction void.

Table 2
Detailed components of the concrete mixtures (mass ratio, dimensionless).

Concrete serial	Binder	Graded quartz sand	Steel fiber	Sand	Aggregate	Water	Rubber powder	Super-plasticizer
1 (1#)	100	–	–	200	200	40		0.4
2 (2#)	100	–	–	200	200	40		0.4
1-1 (3#)	100	–	–	200	200	40		0.3
1-1A (4#)	100	–	–	200	200	40		0.3
HSC 60 (5#)	100			200	200	30		1.0
Imitative RPC (6#)	100	–	–	100	100	18.6	1	1.2
RPC 130 (7#)	100	120	70	–	–	18.0	–	1.6

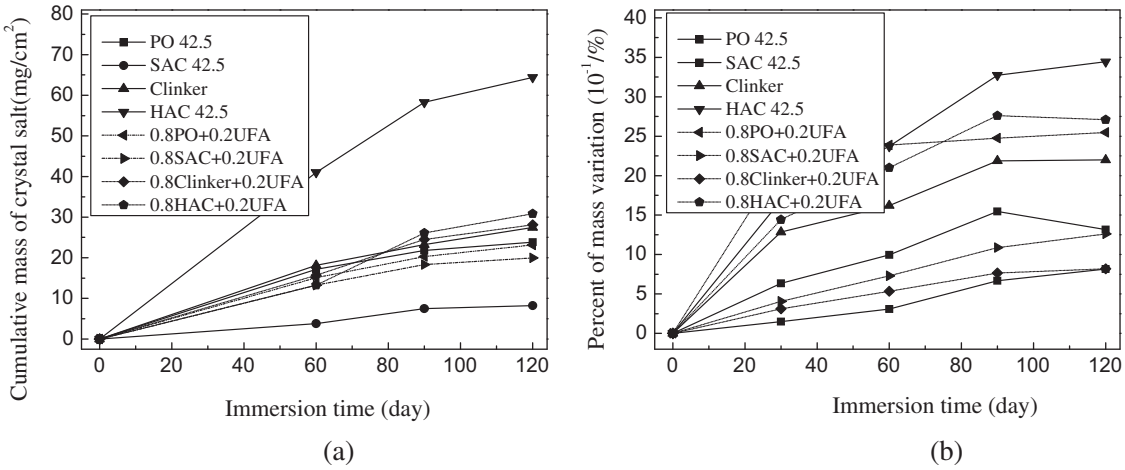

Fig. 1. Properties of (a) salt crystallization and (b) total mass variation.

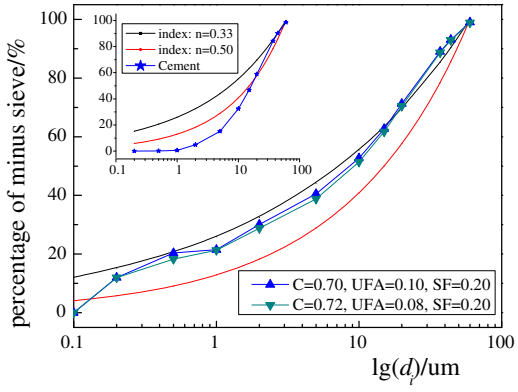

Fig. 2. Optimization of the granular size distribution.

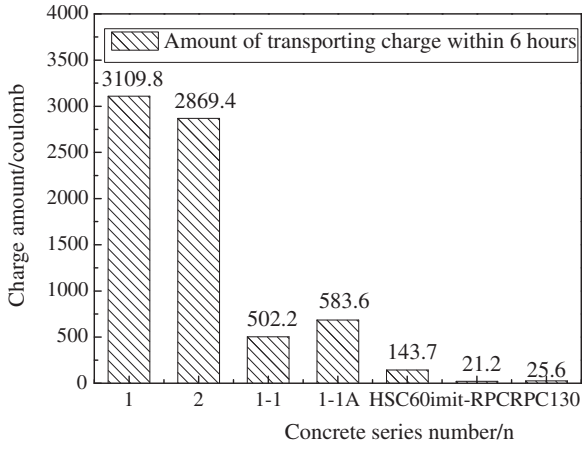

Fig. 3. Properties of chlorine penetration.

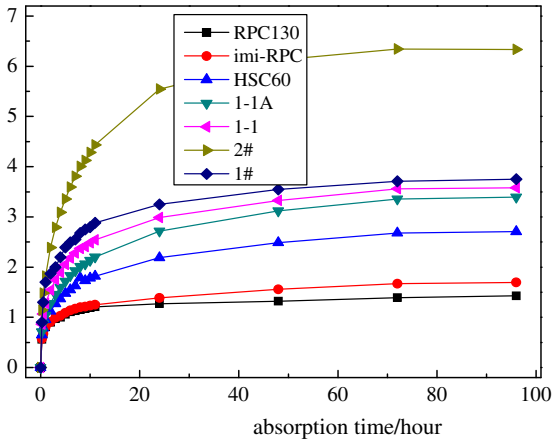

Fig. 4. Properties of absorbing salt solution.

3.2. Penetration and absorption

Figs. 3 and 4 are permeability and absorption results of concrete series at 7-day age. In Fig. 3, the electric flux of imitative RPC was 21.2 C, accounting for around 0.7% of the fiducial concrete serial. The electric flux is extremely low to be comparable with RPC 130. According to ASTM C1202-97, the grade of chloride ion penetration is impenetrability. The permeability of sulphoaluminate concrete has an equivalent grade to that of ordinary Portland concrete and its electric flux within 6 h was slightly below. For control groups, addition of ultrafine mineral powder leads to a sharp reduction of the penetration; therefore, the electric flux is around one sixth of ordinary Portland concrete. Interestingly, the electric flux of polymer-modified concrete is slightly higher than the ultrafine mineral powder modified concrete. Result of salt absorption solution collaborated well with the result of penetration tests. Implied by Fig. 4, the amount of salt solution absorption increased sharply in the first several hours and slowed down gradually. When the absorption equilibrium was reached, it suspended the absorption according to the outside environment. The total salt solution absorption is ranked as the ordinary concrete > the ultrapulverized fly ash concrete > the polymer-modified concrete > HSC 60 > RPC 130 > the imitative RPC.

3.3. Properties to sulphate solution leaching

In order to simulate the deterioration of tunnel lining concrete for sulphate attack, the selected concrete series were subject to unilateral-leaching in sodium sulphate solution. The experiment was conducted with following procedures. Firstly, the specimens were excavated by a power drill and sealed their bottoms by epoxy resin. Then, the treated cubes were covered with a piece of glass after its inner cavity filled with 150,000 ppm sodium sulphate solution. Afterwards, the prepared specimens were stored in creep room with the temperature at 20 ± 2 °C and the relative humidity at 0.5–0.6.

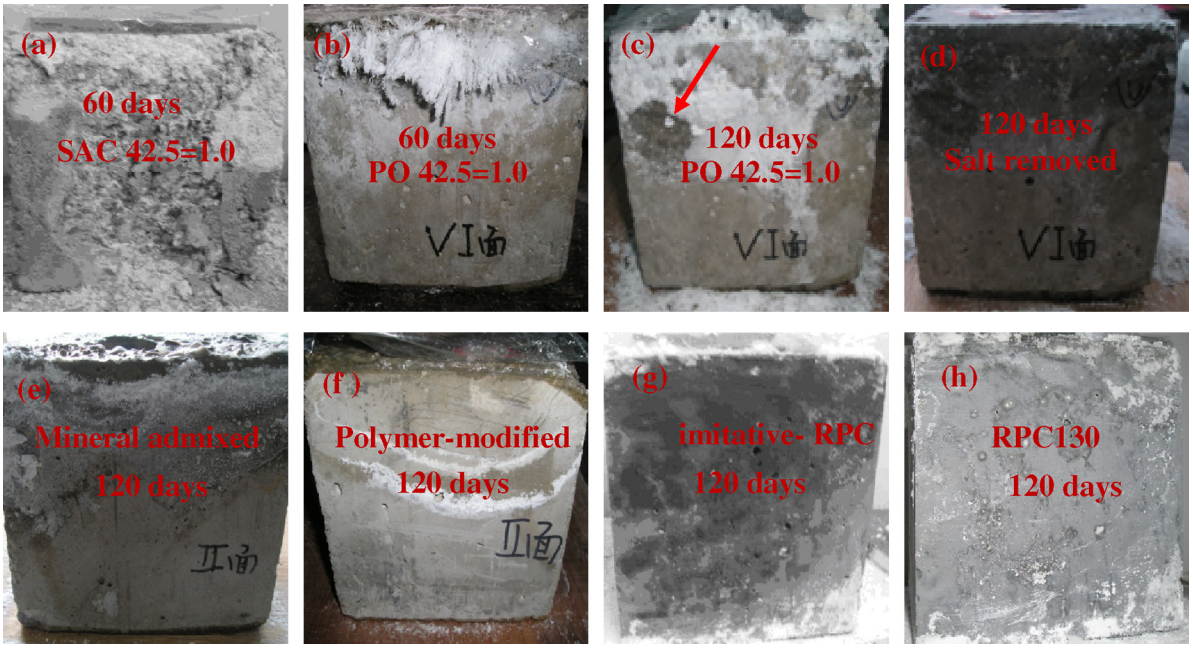

Fig. 5. Leaching in 150,000 ppm sodium sulphate solution.

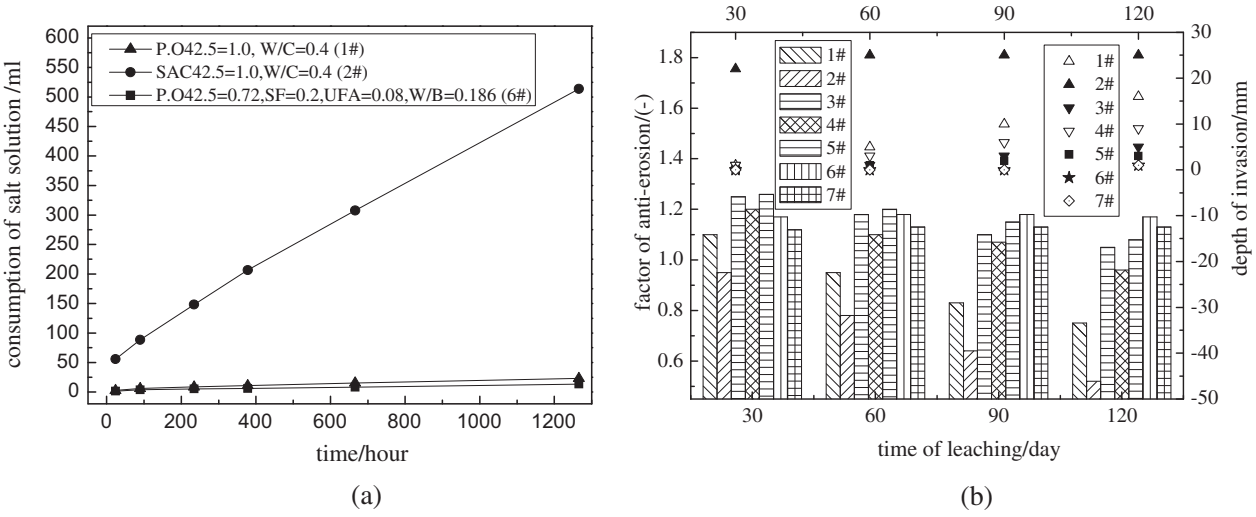

Fig. 6. Results of the unilateral leaching test. (a) Sodium sulphate solution consumption and (b) anti-erosion factors and depth of invasion.

Fig. 5 shows the salt crystal and classic appearance disintegration of concrete unilateral-leached in sulphate solutions for 120 days. It can be seen that some well growth deterioration occurred to the three reference ordinary concrete serials for salt crystallized in the upper zone of the four mold surfaces. The sulphoaluminate ordinary concrete serial has the worst deterioration. Salt crystals were spotted on surface of the sulphoaluminate ordinary concrete cube (see Fig. 5(a)). The surface layer of concrete was cracking, spalling and then flaking off the matrix after 60 days of unilateral immersion. From Fig. 5(b)–(d), it can be seen visible salt crystals and its spalls the capillary adsorption zone around leaks of the Portland ordinary concrete specimens after 120 days of unilateral leaching age. When the crystallized salt is removed, it can be seen that the geometric dimension and quantity of capillary increased greatly. The ultra-pulverized fly ash concrete serial and the polymer-modified concrete serial demonstrated better performance in salt crystallization than the Portland ordinary concrete serial (see Fig. 5(e) and (f)). The imitative RPC and RPC 130 exhibit excellent resistance to sulphate attack. It is expounded in several aspects. For example, the geometric shape of specimens retain intact (see Fig. 5(g) and (h)), and surfaces were clean and compacted, nothing but a little salt crystallized on the mold surface. Meanwhile, the depth of invasion extremes shallow after having been leached in sodium sulphate solution for 120 days.

Fig. 6 shows specimens unilaterally immersed in 150,000 ppm sodium sulphate solution. The consumption of salt solution is monitored by a graduated glass tube connected with the cavity of concrete cylinder. Solution consumption of concrete serial named the Portland ordinary concrete (1#), the sulphoaluminate ordinary concrete (2#) and the imitative reactive powder concrete (6#) was presented. It can be seen that the salt solution consumption of sulphoaluminate ordinary concrete serial is far larger than that of the Portland ordinary concrete serial and the imitative RPC serial. The solution consumption between the Portland ordinary concrete serial and the imitative RPC serial is equivalent, and the Portland ordinary concrete serial has slightly more consumption of the

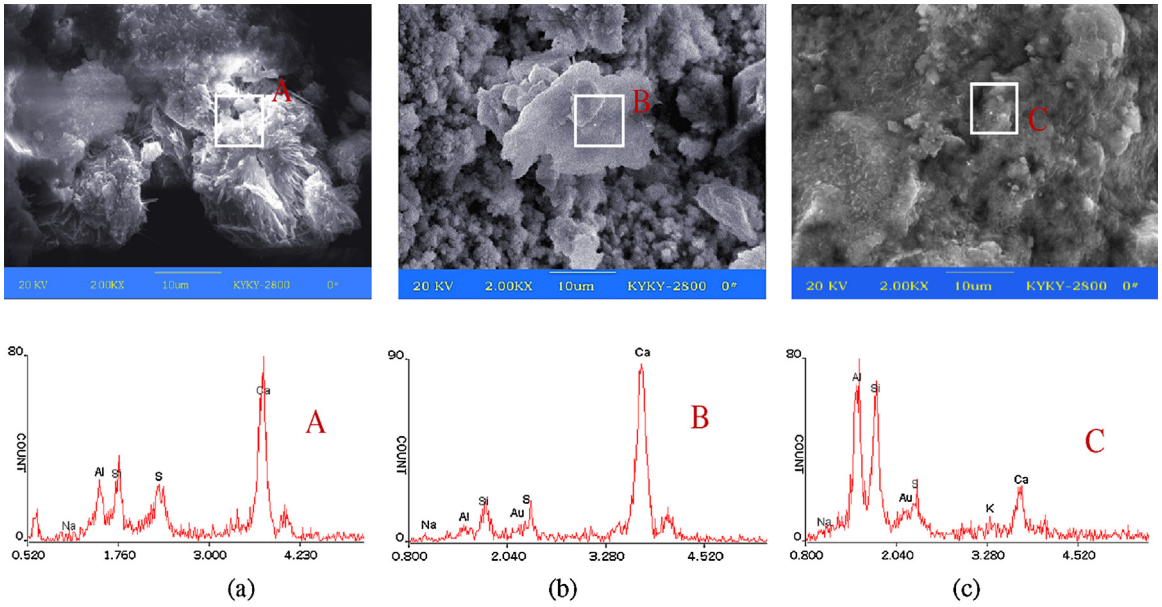

Fig. 7. SEM images and EDS spectrum of various serials. (a) Ordinary concrete, (b) mineral admixture concrete and (c) reactive powder concrete.

sodium sulphate solution. In Fig. 6(b), the sulphoaluminate ordinary concrete serial has the maximum invasion depth and the least factor of anti-erosion to sulphate leaching. The specimens using sulphoaluminate cement have been penetrated during 60 days of leaching and the degradation of concrete decreased to 40% after 120 days of sodium sulphate solution leaching. Ordinary cement concrete serial exhibits better performance than sulphoaluminate ordinary concrete with same water to cement ratio by sulphate leaching attack. If content of cement is replaced by equal silicon aluminum material in concrete with low water to cement ratio, the resistance to sulphate leaching attack would improve greatly. The imitative RPC and RPC 130 have outstanding performance to sulphate leaching attack, its depth of invasion extreme shallow and the factor of anti-erosion retains above one point one after 120 days of leaching time.

4. Discussion

The imitative RPC material mixed with high content of silica fume and with extremely low water to cement ratio. The pozzolanic effect combined with the packed hydration distance contributes greatly to the excellent performance to sulphate attack by greatly decreasing the porosity of concrete, especially reduction in the aperture and quantity of capillary [12]. Such great changes then effectively hindered the rapid transportation of sulphate ions and the consumptions of portlandite, restrained the production of ettringite and calcium sulphate. Firstly, the appropriately gradated particles of cement, fly ash and silica fume extend the gradation range and reach the maximum bulk density. Then, the complementary of silica fume and fly ash improves the hydration condition and initiates application of pozzolanic [13–15]. In this section, the content of calcium hydroxide sounds very important. For example, The P.O 42.5 and the ground Portland cement clinker generated abundant calcium hydroxide in hydration. The high alkali environment leads to unreserved secondary pozzolanic reaction. Conversely, SAC 42.5 serial and HAC 42.5 serial belong to low alkaline cement, addition of silica-aluminum materials enlarged the w/c ratio and complicated the simulation of pozzolanic activity. The secondary C-S-H deposited in the pores thereby made concrete close-grained and impermeable, and therefore, blocked the penetration paths for sulphate ions through the concrete matrix [16–18]. Furthermore, the fine aggregates act as the skeleton and the inert filler. It can reduce the cement content per cube and restrain cracking [19]. As a result, the price of concrete per cube is reduced besides enhancing the impermeability for aggressive ions.

SEM image and energy spectrum expound excellent performance of the imitative RPC materials to sulphate attack. Images and energy diagrams selected from the Portland ordinary concrete (denoted by 1# or 5#), the mineral admixed concrete (denoted by 3# or 4#) and the imitative RPC materials (denoted by 6#) were shown in Fig. 7. It can be seen that the microstructure of Portland ordinary concrete differed obviously from that of mineral admixed concrete and the imitative RPC materials. Seen from the image of 1# concrete, there are many erosion products due to the reaction between hydration calcium aluminum, portlandite and sodium sulphate. The flaky ettringite and calcium sulphate gathered into clustered mass. These hydration products and sodium sulphate from environmental solution for leaching separated from aperture solution produced a large expanding force in concrete and, therefore, resulted in the severe degradation of properties. In image of 1-1#, there are only hydration products of C-S-H, portlandite and the fly ash fine pellets can be seen. The hydration gels and fine fly ash granules are packed so densely that no growing space was left for ettringite and gypsum development. For polymer-modified concrete serial (1-1A#), the re-polymerized polymer blocked some capillaries and simply weakened the pozzolanic reaction of mineral additives. No one can hardly distinguish the polymer-modified concrete serial (1-1A#) from the mineral admixed concrete serial (1-1#). In SEM image of the imitative RPC sample, the fly ash pellets were buried or wrapped with hydrate/secondary C-S-H gels vastly.

5. Conclusions

The stable and compact geometrical interior structure-liked contents of hydration gels hindered the rapid transportation of ions in sodium sulphate solution and, therefore, endowed the imitative RPC materials with qualified performance in sulphate environment. Compared to conventional RPC, introduction of mineral aggregate and rubber powder contents leads to minor shrinkage when enhanced flexibility, especially the reduction of expensive contents

makes the imitative RPC ever more affordable. In summary, the imitative RPC material displayed excellent retrofit potentials on economic feasibility and with high impermeability and excellent durability to sulphate attack.

Acknowledgments

Funding for the project was obtained from the Key Technology Research and Development of Railways Ministry project (item serial number: 2008 G 025-C). The skill and cooperation of each of these units and individuals were appreciated by the authors.

References

[1] P.-C. Aïtcin, Cements of yesterday and today: concrete of tomorrow, Cem. Con. Res., 30, 1349–1359 (2000).
[2] R. Pieer and C. Marcel, Composition of reactive powder concrete, Cem. Con. Res., 25, (7) 1501–1511 (1995).
[3] M. An, Q. Wang and J. Ding, Reactive powder concrete batching principle and application prospective, Archi. Tech., 32, (1) 15–16 (2000).
[4] Y. Xie, B. Liu and G. Long, Study on reactive powder concrete with ultra-pulverized fly ash, J. Build. Mater., 4, (3) 280–284 (2001).
[5] V. Matte, C. Richet and M. Moranville, Characterization of reactive powder concrete as a candidate for the storage of nuclear wastes Symposium on High Performance and Reactive Powder Concretes, vol. 3, Sherbrooke, Canada, (1998) pp. 75–88.
[6] H. Bai and R. Gao, The application of railway reactive powder concrete in engineering construction, Build. Sci., 19, (4) 51–54 (2003).
[7] B. Behloul and K.C. Lee, Ductal® Seonyu footbridge, Struct. Con., 4, (4) 195–201 (2003).
[8] D. Btienne, M. Causse, M. Behlow et al., Design and building of Seoul Peace footbridge Third International Arch Bridge Conference, vol. 9, Paris, (2001) pp. 865–876.
[9] D. Bierwagen, A.A. Hawash, Ultra High Performance Concrete Highway Bridge. http://120.52.72.38/www.ductal.com/c3pr90ntcsf0/52-Wapello_Bridge_Paper.pdf.
[10] J. Li, Study on Properties of Ultra-Fine Powder of Reactive Powder Concrete, Harbin Institute of Technology, Heilongjiang (2001).
[11] S. Yuenan, Particle combination of fine powder effect on performance of cement and concrete, Harbin Institute of Technology (2008), pp. 10.
[12] Y. Xie, X. Tang and G. Long, Experiment on cement-based materials with various compositions against sulfate attack, Adv. Mater. Res., 168–170, 94–98 (2011).
[13] J Li, The Mix Proportion Design and Application Research of RPC130, Shijiazhuang Tiedao University, Hebei (2012).
[14] S. Song and C. Wei, Durability of reactive powder, Concrete, 196, (2) 72–80 (2006).
[15] A. Cwirzen, V. Penttala and C. Vornanen, Reactive powder based concretes: mechanical properties, durability and hybrid use with OPC, Cem. Con. Res., 38, 1217–1226 (2008).
[16] G. Long, Y. Xie and M. Shi, Hydration characteristics and microstructure of compound cementitious system with reactive powder, J. Rail. Sci. Eng., 4, (4) 52–55 (2007) (in Chinese).
[17] Q. Zhou, C. Cai and Y. He, Microstructure and strength of reactive powder concrete, J. Chin. Electr. Microsc. Soc., 22, (6) 594–5959 (2003).
[18] A. Korpa, T. Kowald and R. Trettin, Hydration behaviour, structure and morphology of hydration phases in advanced cement-based systems containing micro and nanoscale pozzolanic additives, Cem. Con. Res., 38, 955–962 (2008).
[19] G. Long, Y. Xie and X. Tang, Evaluating deterioration of concrete by sulphate attack, J. Wuhan Univ. Technol. Mater. Sci. Ed., 22, (3) 572–576 (2007).